Preparation and Characterization of Poly(butyl acrylate-*co*-2-ethylhexyl acrylate) Grafting of Vinyl Chloride Resin with Good Impact Resistance

Mingwang Pan, Liucheng Zhang

Institute of Polymer Science & Engineering, School of Chemical Engineering, Hebei University of Technology, Tianjin, 300130, People's Republic of China

ABSTRACT: Crosslinked poly(butyl acrylate-*co*-2-ethylhexyl acrylate) [P(BA–EHA)] latex was synthesized by seeded emulsion polymerization. P(BA–EHA)/poly(vinyl chloride) (PVC) composite latex was prepared using P(BA–EHA) latex as the seed. The effects of the amount of P(BA–EHA) on the latex particle diameters and mechanical properties of the materials are discussed. The grafting efficiency (GE) of P(BA–EHA)-grafted vinyl chloride (VC) in the synthesized resin was investigated, and the GE increased with an increasing P(BA–EHA)/VC ratio. The morphology of P(BA–EHA)/PVC was characterized using TEM, SEM, and DMA. TEM indicated that the particles of the P(BA–EHA)/PVC composite latex have a clear core–shell structure. DMA illustrated that the compatibility between P(BA–EHA) and PVC was well improved. With an increasing P(BA–EHA) content, the loss peak in the low-temperature range became stronger than that of pure PVC, and the maximum values of the loss peaks gradually shifted to higher temperature. SEM showed that the fractured surface of the composite sample exhibited better toughness of the material. The notched impact strength of the material with 4.2 wt % P(BA–EHA) was 11 times that of PVC. TEM showed that P(BA–EHA) was uniformly dispersed in the PVC matrix and that the interface between the two phases was indistinct. © 2003 Wiley Periodicals, Inc. J Appl Polym Sci 90: 643–649, 2003

Key words: poly(vinyl chloride) (PVC); emulsion polymerization; core-shell polymers; impact resistance

INTRODUCTION

Poly(vinyl chloride) (PVC), obtained by the emulsion polymerization technique, has been widely applied in buildings, indoor decoration, toys, electrical appliances, instrument panels, articles of everyday use, etc. The notched impact strength of PVC resin made by suspension or emulsion polymerization is low. So, impact-resistant modification for PVC resin has been extensively studied. Many polymers or copolymers are used as impact-resistant modifiers of PVC such as chlorinated polyethylene (CPE), methyl methacrylate–butadiene–styrene (MBS), and polyacrylate (ACR). ACR, as an impact modifier and processing aid of thermoplastic resins like PVC, is much welcome because of its excellent elastic and antiaging properties.[1–6]

Adding a crosslinked rubbery polymer into PVC resin is a conventionally used method for PVC modification. But there are some deficiencies such as comparatively poor compatibility and phase separation between PVC and poly(acrylic ester), so the crosslinked rubbery polymer is not uniformly dispersed in the PVC matrix. In this article, a series of composite latices were synthesized by the grafting of vinyl chloride onto crosslinked poly(butylacrylate-*co*-2-ethylhexyl acrylate) [P(BA–EHA)] latex.[7–10] The effects of the P(BA–EHA) level on the particle diameters of the P(BA–EHA)/PVC composite latex and the mechanical properties of the corresponding materials were intensively investigated. The miscibility between P(BA–EHA) and PVC was characterized by dynamic mechanical analysis (DMA). The morphological structure of the composite latex particles and the material was studied by transmission electron microscopy (TEM). The morphology of the failure surfaces for the notched samples was observed by scanning electron microscopy (SEM). Here, a new variety of PVC resin with good impact resistance and some other improved properties was obtained by seeded emulsion polymerization.

EXPERIMENTAL

Materials

The monomers, *n*-butyl acrylate (BA), 2-ethylhexyl acrylate (EHA), and 1,4-butylene glycol diacrylate (BDA), were industrial products. All the monomers were supplied by the Beijing Dong Fang Chemical Plant (Beijing, China), freshly distilled under a vac-

uum and stored at −10°C prior to use. Sodium dode-cylsulfate (SDS), chemically pure, was used as an emulsifier. Potassium persulfate ($K_2S_2O_8$), chemically pure, recrystallized by distilled water at 35°C, was used as an initiator. Sodium tetraborate ($Na_2B_4O_7$), chemically pure, was the pH modifying agent. Vinyl chloride (VC), above 99.99 wt % purity, was supplied by the Tianjin Chemical Plant (Tianjin, China). Calcium stearate, stearyl alcohol, chemically pure, and an organotin stabilizer were commercial grade and supplied by the Tianjin Chemical Co.

Synthesis of P(BA–EHA) latex

Distilled water, 200 mL, SDS, 0.50 g, BA, 12.9 g, EHA, 5.6 g,, BDA, 0.28 g, and $K_2S_2O_8$, 0.15 g, were charged into a 500-mL four-necked glass flask. The mixture was stirred and purged under nitrogen for over 20 min. Then, 37 mL of a $Na_2B_4O_7$ solution, with a concentration of 0.03 g/mL, was added to control the pH of the reaction system between 8 and 9. Next, the reaction vessel was heated to 80°C. The copolymerization was carried over 1.5 h under a N_2 atmosphere and stirred thoroughly.

In the second stage, a monomer mixture of 51.6 g of BA, 22.4 g of EHA, 1.11 g of BDA, and 0.30 g of $K_2S_2O_8$ dissolved in 20 mL distilled water was added dropwise over 1.5 h. The reaction was then maintained at 80°C for an additional 2 h.

Preparation of P(BA–EHA)/PVC emulsion resin

A mixture of 900 mL of deionized water, 2.20 g of SDS, and 0.70 g of $K_2S_2O_8$ was charged into a 2-L stainless-steel autoclave, and a certain amount of P(BA–EHA) latex as the seed was added. Five weight percent of the sodium hydroxide solution was used to adjust the pH of the reactive mixture between 9.5 and 10.5. After closing and removing air, 400 g of the VC monomer was gradually introduced into the reactor under stirring. The polymerization was continued at 50 ± 0.3°C until the pressure decreased to 0.35 MPa and the seeded emulsion copolymerization was short-terminated. After cooling, the unreacted monomer was removed. The resin was isolated from the emulsion by freezing at −20°C.The product was filtered, rinsed with deionized water, and dried under reduced pressure at 50°C.

Measurement of latex particle diameter

The particle diameters and their distribution, including the P(BA–EHA) copolymer and the P(BA–EHA)/PVC composite latex, were measured by a Coulter Model N4MD submicron particle analyzer (Coulter Electronics Inc.)

Determination of grafting efficiency (GE)

P(BA–EHA)-grafted VC resin is substantially a mixture which is composed of the homopolymer of PVC, crosslinked P(BA–EHA), and the P(BA–EHA)-grafted VC copolymer. So, the determination of the GE requires separating the PVC homopolymer from the P(BA–EHA)-grafted VC resin.[11–13] This is achieved by extraction with tetrahydrofuran, which removes the PVC which is not grafted onto P(BA–EHA), but the crosslinked P(BA–EHA) and its grafted VC copolymer remain. In the experiment, a weighed amount of the sample was sealed in a special paper bag, placed in a Soxhlet thimble, and extracted with tetrahydrofuran for 24 h. The undissolved polymer was dried, weighed, and again extracted with tetrahydrofuran for additional hours. This process was repeated until no further weight loss was observed. The chlorinity of the undissolved polymer was determined by elementary analysis to calculate the grafted PVC amount. The GE was determined by dividing the amount of PVC which was grafted onto P(BA–EHA) by the total amount of PVC present before extraction. It can be calculated by the following equation:

$$ GE = \frac{a\dfrac{M_1}{M_2}X}{b + a\left(\dfrac{M_1}{M_2}X - 1\right)} $$

where a is the mass of the undissolved polymer; b, the original mass of the sample before extraction; M_1, the VC molecular weight; M_2, the chlorine atomic weight; and X, the chlorinity of the undissolved polymer.

Preparation of composite samples

The synthesized resin was mixed with a determined quantity of additives. The processing recipe was 100 parts of resin, 2.5 parts of organotin, 0.8 parts of calcium stearate, and 0.8 part of stearyl alcohol. All components were first mixed in a high-speed mixer at room temperature and then milled on a laboratory two-roll mill between 170 and 175°C for 7 min. Two- or four-millimeter-thick plates were pressed at the temperature of 180–185°C. The plates were cooled under a cooling press. Dumbbell-shaped samples for the tensile tests were cut from the plates. The size of the samples for the notch impact test was 55 × 6 × 4 mm^3; the notch depth was equal to 1/3 of the thickness of the sample.

Determination of mechanical properties

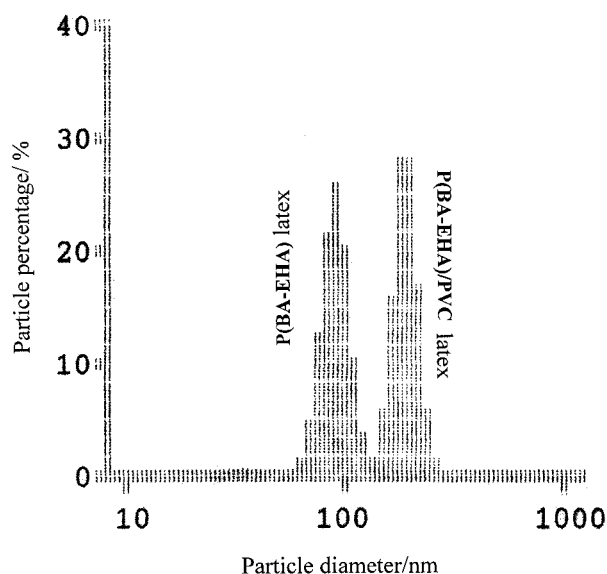Tensile strength testing was performed using an RGT-10A electronic tensile tester with a computer control-

Figure 1 Particle diameter distribution of P(BA–EHA) and P(BA–EHA)/PVC latices. P(BA–EHA) latex: standard deviation (S.D.), 15 nm; MPD, 90 nm. P(BA–EHA)/PVC latex: P(BA–EHA), 6.3 wt % solid; S.D., 26 nm; MPD, 187 nm.

ling system. The test portion of the dumbbell specimen was 25 mm long with a cross section 2×6 mm^2. Tests were conducted at an extension rate of 20.0 mm min^{-1} at 23°C and 50% relative humidity. The notched impact strength was carried out on an XCJ-40 Charpy impact tester.

Dynamic mechanical measurements were carried out using a Netzsch DMA242 (Germany)-type dynamic mechanical analyzer. The measuring frequency was 1 Hz; the heating rate, 3 K/min; and the temperature range, from −10 to +130°C.

Electron microscopy

The morphology of the P(BA–EHA)/PVC samples with the ingredients above-mentioned was characterized by an S-250 scanning electron microscope (SEM). The fractured surface of the notched impact bar was coated with a thin layer of gold under a vacuum. The morphology of the composite latex particles and the rubbery phase in the sample was observed through a Hitachi EM-H-800 transmission electron microscope (TEM) in conjunction with the RuO$_4$-staining method.

RESULTS AND DISCUSSION

Latex particle diameters and their distribution

The particle diameter distributions of P(BA–EHA) and P(BA–EHA)/PVC latices are shown in Figure 1. As seen from Figure 1, the particle diameter distribution of the composite latex is similar to that of the P(BA–EHA) latex and shows a relatively narrow single peak,

but the mean particle diameter (MPD) of the composite latex has increased.

When the amount of the P(BA–EHA) latex in the copolymerization system was varied, the MPD of the synthetic composite latex was shown to be a function of the P(BA–EHA) content (Fig. 2). Figure 2 shows that the MPD of the composite latex gradually decreases with an increasing P(BA–EHA) content. With an increase in the amount of P(BA–EHA), the number of latex seeds, used as the VC-grafted polymerization, obviously increase for the same VC amount. So, the MPD of the formed composite latex decreases. However, all the mean particle diameters of the composite latices are much larger than 90 nm, which is the MPD of pure P(BA–EHA) latex. Moreover, the MPD of the prepared PVC latex was only about 78 nm without the P(BA–EHA) latex as the seed. All these would suggest that PVC macromolecular chains grow on the surfaces of P(BA–EHA) emulsion particles and encapsulate them to form core–shell latex particles, as observed in Figure 3.

Morphology of composite latex particles

The morphological structure of the composite latex particles observed by the TEM study is presented in Figure 3. As shown in Figure 3, the morphology of the composite latex particles has, obviously, a core–shell structure. The deep black portion in the core is the P(BA–EHA) rubbery copolymer by RuO$_4$-staining. The light-colored portion in the shell is PVC. PVC macromolecules encapsulated the P(BA–EHA) particles.

Effect of the amount of P(BA–EHA) added on GE

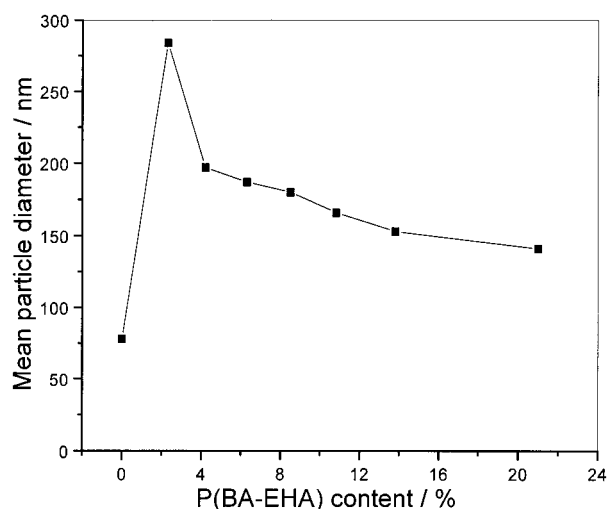Figure 4 shows that the GE increases as the P(BA–EHA)/VC ratio is increased. This was expected. Be-

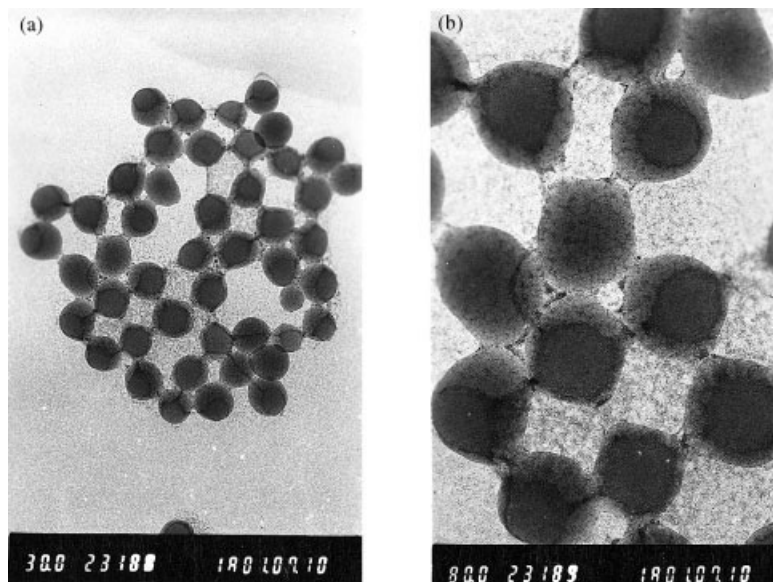**Figure 2** Influence of P(BA–EHA) amount on MPD of the composite latex.

Figure 3 TEM graphs of composite latex particles. P(BA–EHA): 6.3 wt % solid. (a) Magnification: 3×10^4; (b) magnification: 8×10^4.

cause the emulsion polymerization system is heterogeneous, for the same VC amount, by increasing the P(BA–EHA) latex amount, the probability of contact between the VC monomer and the backbone P(BA–EHA) increases. Hence, the probability of grafting VC onto P(BA–EHA) increases. So, the GE is enhanced. Apart from this, it may be attributed to the improved miscibility between the grafted P(BA–EHA) and growing PVC chains which result in an increment in the grafting of VC onto P(BA–EHA).

DMA of resin samples

Figure 5 shows dynamic mechanical spectra of different P(BA–EHA) contents of the resin and pure PVC. As seen in Figure 5, there are two distinct spectral peaks for every curve. There is a wide β-secondary transition peak for the PVC sample; the β-maximum value lies near $-57°C$ at 1 Hz. Compared with pure PVC, the height of the mechanical loss peak of the resin in the temperature range of -45 to $+10°C$ is markedly dependent on the increment of the P(BA–EHA) content. Also, the maximum values of the loss peak positions gradually shift to higher temperature with an increasing P(BA–EHA) content. The experimental data are -56.9, -43.2, -18.0, and $-12.4°C$, corresponding to PVC, and samples 1–3, respectively. This difference might be related to the diffusion of the VC monomer into the crosslinked P(BA–EHA) phase to form the grafting transition layer.
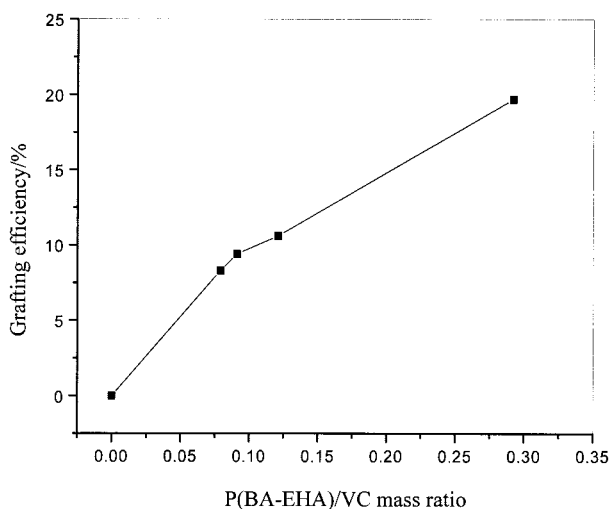

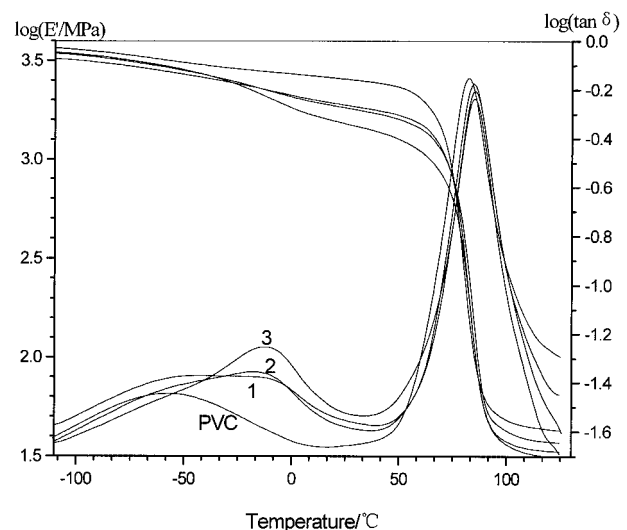**Figure 4** Effect of P(BA–EHA) amount on GE.

Figure 5 Dynamic mechanical spectra of the samples. P(BA–EHA) content: (1) 6.3 wt %; (2) 8.5 wt %; (3) 13.8 wt %.
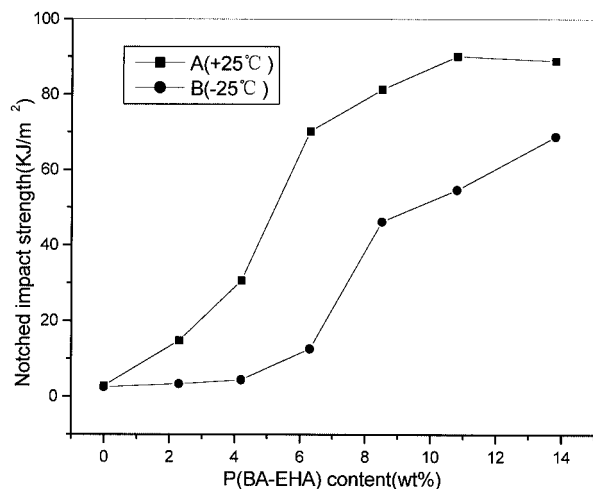
Figure 6 Influence of P(BA–EHA) content on notched impact strength of the materials.

The low-temperature transition of the resin is attributed to the glass transition of the P(BA–EHA) rubbery polymer and the β-secondary transition of PVC chains. The glass transition temperature (T_g) of viscous-elastic P(BA–EHA) is $-47.9°C$ through DSC measurement. The experimental value was higher than the T_g of pure PBA ($T_{g'}$ $-55°C$) or PEHA ($T_{g'}$ $-85°C$) in the literature. This discrepancy may be caused by the higher degree of crosslinking in P(BA–EHA).

The dynamic mechanical spectra demonstrate that the maximum position of the loss peak either in the low-temperature range or in the high-temperature range is different from that of P(BA–EHA) and pure PVC. For the same amount of the VC monomer, the greater the amount of the P(BA–EHA) feed, the greater is the number of P(BA–EHA)/PVC composite particles. Then, the increased GE gives rise to an increased T_g of the resin in the low-temperature transition region, namely, the distance between the maximum values of two tan δ loss peaks in the low- or high-temperature range becomes shorter. DMA results imply that the compatibility between P(BA–EHA) and PVC should have been improved.

Effect of P(BA–EHA) content on impact strength of the material

Figure 6 presents the impact strength results of the materials with varying P(BA–EHA) content. As Figure 6 shows, the notched impact strength of the materials greatly increases with an increasing P(BA–EHA) content whether at low temperature or atmospheric temperature. Wu[14] and Dompas and Groeninckx[15] claimed that substantial enhancement of the toughness of brittle or notch-sensitive polymers can be achieved by dispersing rubber particles in the polymer

matrix. In pseudoductile thermoplastic matrices, which deform preferentially by shear yielding, the major toughening mechanisms are thought to be cavitation of the rubbery particles and shear yielding of the matrix. The transition from brittle to ductile behavior in rubber-modified pseudoductile thermoplastics occurs at a critical value of the interparticle distance (IPD), which is given by the following:

$$IPD = d_0\{(\pi/6\phi_r)^{1/3} - 1\}$$

where d_0 is the particle diameter of the rubber particle, and ϕ_r, the rubber volume fraction. In this article, the MPD of the rubber particles is the same (90 nm). When the rubber content is less than 4 wt % of the material, the interparticle distance is greater than the IPD (122 nm). Then, shear yielding of the matrix does not occur easily and the toughness of the material is not improved markedly.

Here, the P(BA–EHA) elastomer is a pliable component in the materials. When this material is subjected to impact force, according to the "craze-shear band" theory, the rubbery particles become centers of stress concentration and initiate crazes or shear bands. While crazes or shear bands occur and grow, a large amount of energy is absorbed in this region. On the other hand, these pliant particles and the interaction between crazes and shear bands can confine the development of crazes and prevent crazes becoming cracks from the break of materials. Then, the greater the P(BA–EHA) content is, the more crazes and shear bands the rubber particles will initiate. Thus, more energy will be absorbed and the impact strength of the materials will be greatly enhanced.

Macho et al.[16] explained the experimental results from both the brittle strength and the tendency to slip (i.e., the shear strength). They thought that when elastomeric particles are present as a filler they stretch under the applied strength, thus dissipating much of the energy necessary to develop new surfaces of the crack. If a greater amount of filler is applied, the shear strength (the tendency of polymer domains to slip) is decreased so much that a brittle appearance of tough PVC can totally turn elastic. A decrease in toughness above a certain content of the elastomer (9.5 wt %) shows an increase of the elastic properties of tough PVC due to the nature of the elastic properties of the elastomer.

Influence of P(BA–EHA) content on tensile strength and elongation at break of the materials

The influence of the P(BA–EHA) content on the tensile strength and the elongation at break of the materials is shown in Figure 7. As seen from Figure 7, the tensile strength of the materials decreases with an increasing
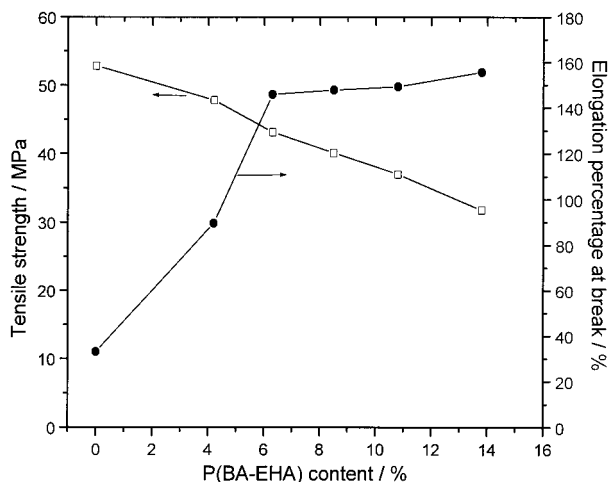
Figure 7 Influence of P(BA–EHA) content on tensile strength and elongation at break of the materials.

Figure 9 SEM photograph of the fractured surface of the composite sample. P(BA–EHA) content: 6.3wt%.

P(BA–EHA) content, but the elongation at break of the materials increases. While the notched impact strength of the material with 4.2% P(BA–EHA) is enhanced to almost 11 times that of pure PVC, its tensile strength is approximately 90% of the tensile strength of pure PVC, and the elongation percentage at break is about three times that of PVC.

SEM and TEM analyses

A TEM graph of the composite sample, which was cut into slices and stained, is shown in Figure 8. Figure 8 shows that the morphology of the material has a two-phase structure with microphase separation. The morphology is consistent with the result of the DMA for
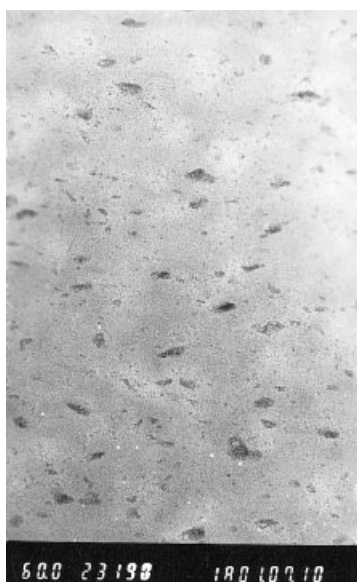
the resin sample. The black portion in Figure 8 is the P(BA–EHA) rubbery polymer stained by RuO_4. Compared with the usual blend modification, the P(BA–EHA) rubbery phase in this system is more uniformly dispersed in the PVC matrix. This good distribution may stem from PVC macromolecules encapsulating the P(BA–EHA) rubbery particles. Then, the coagulation or aggregation among the P(BA–EHA) rubbery particles cannot occur. Because of the presence of the P(BA–EHA)-grafted VC copolymer and that the GE increases with the rubbery copolymer, the compatibility between the two phases was improved and the interface between P(BA–EHA) and PVC is indistinct.

The SEM graphs of the impact breaking surfaces of the P(BA–EHA)/PVC composite and pure PVC samples are shown in Figures 9 and 10, respectively. Figure 9 shows that the fractured surface of the notched impact sample is not a smooth surface, characterized by a rippled fracture surface with striations, and exhibits plastic shear deformation. There are many holes of different sizes on the breaking surface. An extensive plastic deformation of the matrix is evidenced by the appearance of numerous striations, cavitation, and shear banding as well as voids formed by debonding of some particles from the PVC matrix. So, as shown in Figure 9, the fractured surface of the composite sample is rougher and exhibits better toughness of the material. In contrast, the fractured surface of the pure PVC sample shown in Figure 10 is smooth and clear and shows a poor notched impact property.

Figure 8 TEM photograph of the composite sample. P(BA–EHA) content: 6.3 wt %; magnification: 6×10^4.

CONCLUSIONS

1. The mean particle diameters of the composite latices gradually decrease with an increasing
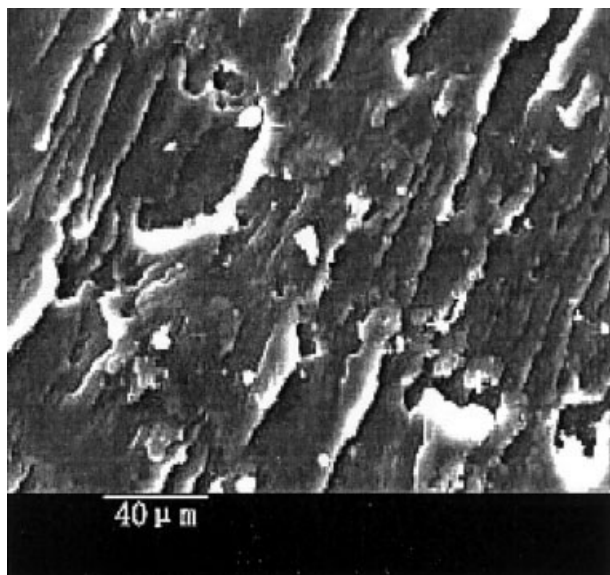
Figure 10 SEM photograph of the fractured surface of pure PVC sample. P(BA–EHA) content: 0.0 wt %.

amount of P(BA–EHA) latex, and PVC macromolecules encapsulate P(BA–EHA) particles to form composite latex particles with a core–shell structure. The GE increases with an increasing P(BA–EHA)/VC ratio.

2. There are two distinct spectral peaks for every resin sample as shown by the dynamic mechanical spectra. Compared with pure PVC, every mechanical loss peak of all the samples is stronger in the low-temperature transition region. Further, the maximum value of the loss peak gradually shifts to a higher temperature with an increasing P(BA–EHA) content. Then, the distance between two loss peaks for every DMA curve becomes shorter. The compatibility between P(BA–EHA) and PVC has been well improved.

3. The notched impact strength and elongation at break of the materials significantly increase with an increasing P(BA–EHA) content, whereas the tensile strength of the materials somewhat decreases. The fractured surface of the notched sample exhibits good toughness. The P(BA–EHA) rubbery phase in the system is uniformly dispersed in the PVC matrix. The morphology corresponds to the very well notched impact property of the material. The developed P(BA–EHA)-grafted VC resin may be industrialized and widely applied for the manufacture of many products in the future.

References

1. Rozkuszka, K. P.; Weier, J. E. U.S. Patent 5 612 413, 1997; Chem Abstr 1997, 126, 278327p.
2. Gao, J.; Yang, L.; Deng, K.; Yao, Z. Polymer 1997, 38, 1139.
3. Zhang, L. C.; Li, X. C.; Liu, T. C. J Appl Polym Sci 1991, 42, 891.
4. Zhang, L. C.; Ren, X. F. J Appl Polym Sci 1992, 45, 1679.
5. Zhang, L. C.; Tai, H. W.; Liu, Y. D. Polym Adv Tech 1996, 7, 281.
6. Zhang, L. C.; Li, X. C.; Liu, T. C. In Three-stage Latex Interpenetrating Polymer Networks; Klempner, D.; Sperling, L. H.; Utracki, L. A., Eds.; Advances in Chemistry Series No. 239; American Chemical Society: Washington, DC, 1994; Chapter 19.
7. Kamimura, A.; Takagi, A.; Yui, K.; Sunakawa, T. Jpn. Patent 11 279 354 A2, 1999; Chem Abstr 1999, 131, 272663b.
8. Fujii, N.; Shinko, T. Jpn. Patent 11 181 033 A2, 1999; Chem Abstr 1999, 131, 74128t.
9. Seiki, A.; Matsumura, K. Jpn. Patent 2000 38 493 A2, 2000; Chem Abstr 2000, 132, 138498u.
10. Huo, J. S. Petrochem Tech 1998, 27, 253.
11. Zhang, X. C.; Wang, L. L.; Qian, B. G. Angew Makromol Chem 1993, 209, 1.
12. Macho, V.; Králik, M.; Micka, M.; Komora, L.; Bakoš, D. J Appl Polym Sci 1998, 68, 649.
13. Zhou, Z. M.; Zhu, M.; Wu, X. D.; Qian, D. Z. Polymer 1994, 35, 2888.
14. Wu, S. Polym Int 1992, 29, 229.
15. Dompas, D.; Groeninckx, G. Polymer 1994, 35, 4750, 4760.
16. Macho, V.; Králik, M.; Micka, M.; Komora, L.; Srokova, I. J Appl Polym Sci 2002, 83, 2355.